A Wide-Range High-Voltage Capacitance Bridge with One PPM Accuracy

OSKARS PETERSONS AND WILLIAM E. ANDERSON

Abstract—**An impedance bridge for high-voltage capacitance and related measurements to an accuracy of 1 ppm is described and the background research and development which made it possible is documented. The bridge is of the transformer-ratio-arm type, the principal components of which are a comparator and several two-stage transformers. The bridge can be used to measure capacitance ratios over a range from 1/1 to 10^7/1 with a resolution between 0.1 and 0.25 ppm. The highest accuracies are obtained at the principal power frequencies of 50–60 Hz, but the bridge is usable up to 400 Hz. The factors which limited the accuracy of previously developed bridges of this type were reexamined and their influence reduced. Two independent methods were developed for the calibration of the bridge.**

INTRODUCTION

HIGH-VOLTAGE capacitance and related measurements require impedance bridges with a large ratio range and continuous adjustment. High-voltage standard capacitors are very expensive and available with only a limited range of capacitance values, typically between 50 and 1000 pF. Laboratories seldom have more than one or two such standards. However, capacitors to be measured come in a large range of capacitance values which are rarely simple multiples of the standard capacitor. The entire flexibility, therefore, must be provided in the impedance bridge, which compares the unknown sample with the standard. Since corrections are difficult to apply to the readings of a multirange bridge, direct reading accuracy is highly desirable.

Several research and industrial applications require 60-Hz measurement accuracies of the order of 10 to 50 parts per million (ppm) and in a few cases as high as 1 ppm, especially for the dissipation factor (DF). A high-voltage bridge based on the current comparator principle with 10-ppm accuracy was first described in [1], [2]. Since then, commercial instruments of this type have become available, and national standards laboratories, including the National Bureau of Standards (NBS), are occasionally requested to calibrate them or verify their accuracy. The development of a new bridge with a 1-ppm direct-reading accuracy was conducted to satisfy the in-house research and measurement needs and calibration requests from outside, and to advance the state of art of low-level multirange current comparators. While transformer-ratio-arm bridges with a limited ratio range but better than 0.1-ppm accuracy have been constructed, especially for operation as voltage transformer bridges [3], the required accuracy in a wide-range instrument with continuous ratio adjustment could not be achieved with the previously developed techniques.

In the development of this bridge, the two basic types of current comparator errors—magnetic and capacitive—had to be reexamined and reduced. The overall bridge is a complex instrument consisting of a number of precision transformers. The uncertainties of critical individual components are maintained at a few tenths of a ppm to obtain the overall system accuracy of 1 ppm. The transformers are constructed and interconnected utilizing two-stage techniques. The ancillary electronic circuits are designed to be compatible with the overall accuracy requirements.

Two methods were developed for the calibration of the bridge. The first, based on a linear transformer-type network, was employed to check the transformers before they were installed in the bridge assembly. The second method utilizes a group of capacitors as transfer standards of ratio. The complete bridge was calibrated by a self-contained buildup procedure.

This paper emphasizes the steps that were taken to achieve the required accuracy and to verify the performance of the bridge. It omits the construction details, which are available in [4].

OPERATING PRINCIPLES

The bridge circuit in its elementary form is shown in Fig. 1. The currents from the two admittances to be compared ($j\omega C_x + G_x$ and $j\omega C_s$) are passed in the ratio windings (N_1 and N_2) of the current comparator and the number of turns is adjusted until ampere-turn balance as indicated by zero signal in the detection winding is achieved. The current for balancing the equivalent loss component of the unknown capacitor is generated by the amplifier circuit, which is similar to that of the previous design [1].

Assuming ideal transformers and amplifiers, at bridge balance the impedances are related as follows:

$$C_x = (N_1/N_2)C_s \tag{1}$$

$$G_x = (N_1/N_2)(C_s/C_f)\alpha G_s. \tag{2}$$

It is customary to express the loss component as the DF or tangent of the loss angle (δ). In these terms, the bal-

Manuscript received July 4, 1975. This paper is partly based on a dissertation submitted by O. Petersons to the School of Engineering and Applied Science, George Washington University, Washington, D. C., in partial fulfillment of the requirements for the D.Sc. degree.

The authors are with the Electricity Division, National Bureau of Standards, Washington, D. C. 20234.

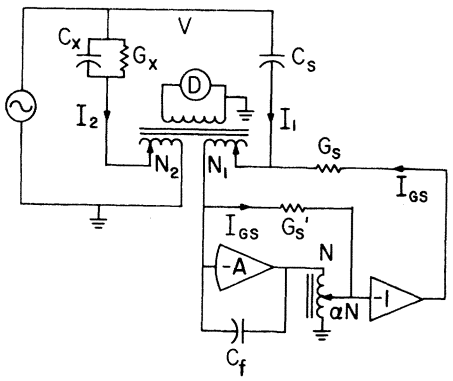

Fig. 1. Basic high-voltage–capacitance bridge.

ance equation becomes

$$\mathrm{DF} = \tan\delta \equiv (G_x/\omega C_x) = \alpha(G_s/\omega C_f). \qquad (3)$$

The bridge is made direct reading by adjusting N_1 as a decimal fraction of the total number of turns by means of decade switches. N_2 is adjusted in coarse steps for range multiplication. The ratio of the autotransformer in the amplifier circuit is also adjusted as a decimal fraction. Since $G_s/\omega C_f$ is constant and any convenient value can be selected, the bridge can be made direct reading also in dissipation factor for any particular frequency. Note the presence of two standard conductances, G_s and G_s', which are of the same value. G_s' prevents second-order errors in the bridge reading; without it the bridge would not be exactly direct reading. By interchanging the connections between the conductances and the inverting amplifier, the bridge can measure equivalent negative dissipation factors. This is a necessary feature if the unknown capacitor has lower losses than the standard. It is also required when the bridge is used to measure voltage transformer ratios.

A more extensive schematic diagram which includes all the major components of the actual bridge is shown in Fig. 2. The current comparator (TR1) is a two-stage transformer. For capacitance ratios larger than 100/1, autotransformer (TR2) is cascaded to the current comparator to increase the overall ratio to 1000/1. A separate primary winding on this range extending transformer further increases the bridge ratio to 10^4/1. TR2 is permanently installed in the bridge enclosure. Still larger ratios, up to 10^7/1, are obtained with the second range extending transformer (TR3). This is an external feedthrough-type current transformer. It has permanent 1000-turn secondary and 100-turn primary windings. Other primary windings can be placed on as feedthrough turns. Although it is not shown in the diagram, the two range extenders are two-stage transformers, the details of which are discussed later.

The bridge has a seven-decade adjustment for the capacitance ratio which with a proper use of the multiplier settings yields a resolution between 0.1 and 0.25 ppm. Since the winding N_1 has nominally only 100 turns or two decades of adjustment, a five-decade inductive divider (TR4) is cascaded to N_1. The two most significant decades of the divider are in a two-stage transformer.

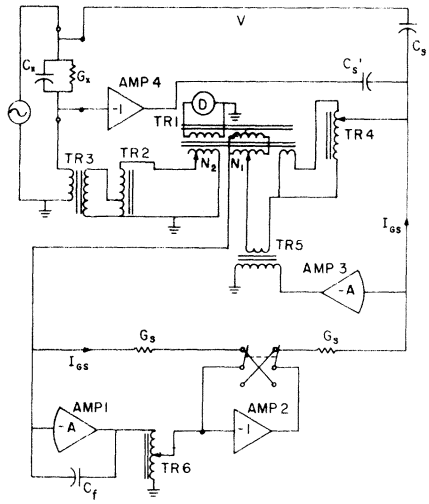

Fig. 2. Complete bridge.

Large unknown capacitors must be measured as four-terminal elements since the lead impedances are significant. Such measurements are realized by means of a previously described [2] lead compensator consisting of an inverting amplifier (AMP4) and a capacitor C_s' of the same value as C_s. The bridge is also compensated for the internal impedance of the windings on the C_s side of the bridge. This impedance is reduced with negative feedback involving the amplifier AMP3 and transformer TR5. This compensating circuit permits the connection of the relatively high conductance, G_s to the transformer winding without the introduction of a significant error.

THE NATURE OF BRIDGE ERRORS AND THEIR REDUCTION

The three components of the bridge whose errors enter directly into the overall system error are the current comparator and the two range extenders. It has been recognized that the principal errors of current comparators and related transformers are of magnetic and capacitive origin [5]. When magnetic error is present, zero signal in the detection winding does not correspond to ampere-turn balance in the ratio windings. Magnetic error is associated with magnetic leakage—the flux which is at least partly external to the magnetic core but which couples into the detection system. Capacitive error arises because a part of the current intended for the ratio windings bypasses them because of internal capacitances. Other potential sources of error are the magnetizing currents in the range extending transformers, system noise, electromagnetic coupling of ambient fields, and the electronic circuits.

A. Magnetic Error

The initial attempt to construct a current comparator with better than 1-ppm accuracy was unsuccessful; magnetic errors which could not be explained on physical bases were observed. For example, the errors could be increased by making the ratio windings skew; the

current comparator was sensitive to a magnetic field in the direction of the major axis of the toroidal core. As a result, a systematic investigation of the sensitivity of current comparators to external (leakage) magnetic fields was undertaken.

Consider a conceptual current comparator as in Fig. 3. The detection winding is wound uniformly on the core. Loops 1 and 2 are the ratio windings, while loop 3 is an external current loop. The transfer impedances z_{41} and z_{42} differ by a small amount and the normalized difference is the error of the current comparator for this particular winding configuration. The signal in the detection winding is induced not only by the flux which is confined entirely to the core, but also by the leakage flux. The causes of this sensitivity to external fields can be nonuniformities in the distribution of the detection turns, imperfections in the geometry of the toroidal core, and inhomogeneities and anisotropies in the magnetic material. This and previous experimental investigations have shown that the latter two are the principal causes of the sensitivity to leakage fields [5], [6].

It is neither practical nor necessary to characterize current comparators for the sensitivity to leakage fields produced by every conceivable configuration of ratio windings. It has been found that tape wound cores are particularly sensitive to fields of certain well defined geometries. Such fields can be produced by purely external loops such as the loop 3 in Fig. 3. The ratio of transfer impedances z_{43}/z_{41} can be considered as a measure of the current comparator error for each particular geometry of the external loop.

In particular, three types of leakage fields were found to be important. The first is a cylindrical dipole field [5] produced by two equal and opposite currents parallel with the axis of the toroid as shown in Fig. 4(a). This sensitivity results from unequal permeability of the two halves of the core, the likely causes of which are residual mechanical stresses and temperature differences during the annealing process.

Tape-wound cores are exceptionally sensitive to the radial field perpendicular to the axis of the toroid [6]. Such a field can be produced by two series-connected loops carrying currents in opposite directions as in Fig. 4(b). This sensitivity arises because a part of the flux traversing the core material from the inner to outer radii takes a spiral path along the tape and thus induces voltage in the detection winding.

Finally, the cores are sensitive to fields in the axial direction as produced by the two coils in Fig. 4(c) carrying currents in the same direction. This phenomenon is caused by the exciting flux which passes through the window of the core, and not necessarily through the core material. Such a flux induces voltage in the spiral tape. If the tape is short-circuited by a metallic protective case, a burr along its edge, or generally poor insulation, the ensuing eddy currents can take a path which partly links the core material and thus induces flux in the core and voltage in the detection winding.

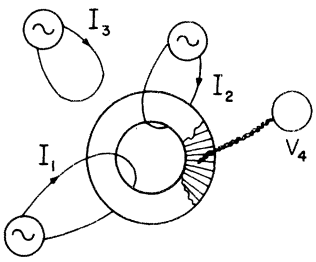

Fig. 3. Core-linking and external current loops.

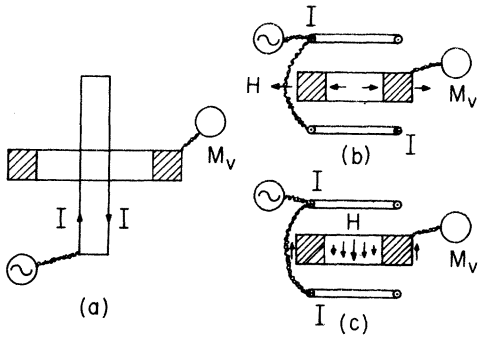

Fig. 4. Testing of current comparators for sensitivity to external magnetic fields.

All three leakage fields can be produced by imperfectly coupled ratio windings; for example, a dipole field, by two windings which are physically displaced on the core; radial and axial fields, by skew ratio windings; axial field by a winding which encircles the axis of the toroid.

It is our practice to test the cores of accurate transformers using the previously described procedures. For the highest accuracy applications only those which are relatively insensitive to axial and dipole fields are selected. Little can be done to control the sensitivity to radial fields since it is an inherent characteristic of the tape-wound construction.

Results for several commercial tape-wound cores and three experimental cores made from annular rings are presented in Table I. The tabulated values are "errors" defined as $\epsilon = z_{43}/z_{41}$ for one-turn external loops of the type shown in Fig. 4. As expected, all tape-wound cores are sensitive to radial fields; the sensitivity is within the same order of magnitude. The sensitivities to dipole and axial fields vary considerably more among cores since these depend on the imperfections of the cores. Annular ring cores are superior to the tape-wound cores. It appears that transformers with errors as low as a few parts in 10^7 could be constructed using ring cores. Unfortunately they are expensive to construct and not commercially available.

B. Magnetic Shielding

The magnetic error can be reduced by close magnetic coupling of the ratio windings. However, such coupling is very difficult if the turns ratio is large, for example, if a single turn is used in one of the windings and 100 turns in the other. Another approach is to use a magnetic shield which prevents leakage fields from being coupled into the detection system. Awareness of the leak-

TABLE I
Sensitivity of Cores to External Fields

Size ID x OD x Ht (cm)	Error (ppm) Type of Field		
	Radial	Axial	Dipole
Tape-Wound Cores			
5.1 x 7.6 x 1.3	19	6	10
5.1 x 7.6 x 1.3	40	1	16
7.6 x 10.2 x 1.3	22	1	12
7.6 x 10.2 x 1.3	16	0	28
5.1 x 7.6 x 2.5	27	11	8
10.2 x 15.2 x 2.5	17	25	6
Annular Ring Cores			
5.1 x 7.6 x 1.1	0.3	0.6	6
5.1 x 7.6 x 1.1	0.3	0.8	4
7.6 x 10.2 x 1.1	0.6	2.0	5

age field patterns to which the cores are sensitive and supporting quantitative data facilitate designing effective shielding enclosures.

Analytical shielding formulas [7] are practical only for geometrically simple enclosures—spheres and long cylinders. While actual toroidal shields only remotely approximate these simple geometries, it is nevertheless advantageous to make seemingly gross approximations and calculate the worst case shielding effectiveness. The analytical approach does provide a firm starting point in the design of efficient and effective shields. Simplified analytical formulas [4] are usually adequate. In the following qualitative discussion the merits of several enclosures are considered.

For shielding against dipole and radial fields, a simple but effective enclosure consists of two U-shaped toroidal channels shown as the layer C in Fig. 5(a). The material is a high-permeability nickel–iron alloy about 1 mm thick. The adverse effect of gaps between the two channels is reduced by large overlaps. Another high-permeability shield is shown in Fig. 5(b). It consists of two tape-wound toroids about 5 mm thick and two sets of annular rings. This shield is poor in radial fields because of the air gaps. Parts D in both shields represent insulating spacers.

Both of these high-permeability shields by themselves are ineffective against axial fields. In principle, shielding could be obtained with a high-conductivity (eddy-current) enclosure such as layer B in Fig. 5(a). However, for power frequency applications the shield has to be very thick, about 1 cm or more, to be of any value. The effectiveness of a thin eddy-current shield can be improved by placing a high-permeability layer on top of it as in Fig. 5(a). Small circular current in the high-conductivity layer induces large flux in the high permeability material. The resultant net flux through the core window as sensed by the detection system is greatly reduced. The shields must be placed on the core in the correct order; a double shield with the reversed order—the high-conductivity material on the outside—is ineffective.

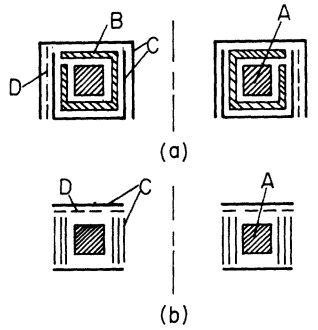

Fig. 5. Magnetic shielding arrangements. (a) Two-layer shield consisting of high-conductivity and high-permeability layers. (b) Magnetic shield constructed from tape-wound toroids and annular rings.

The measured shielding ratios of single and multilayer shields of the type shown in Fig. 5 are listed in Table II. Shields 1 and 3 are high-permeability enclosures constructed as in Fig. 5(a); shield 2 is made from 0.3-cm thick copper; shield 4 is a high-permeability enclosure of the type shown in Fig. 5(b). The tabulated shielding factor is defined as the ratio of the error without the shield to that with the shield.

The results confirm the expected relative merits of various individual enclosures and their combinations; they illustrate the advantages of multilayer enclosures and the necessity for proper ordering of high-conductivity and high-permeability layers; extremely high-shielding ratios are obtained with a three layer shield. The experimental values agreed with those calculated using analytical formulas within a factor of 2 to 3. In view of the many uncertainties and assumptions involved in the calculations, this agreement is considered good.

The magnetic error was also measured for the worse case configuration of ratio windings. Two concentrated windings were placed on the core 180° apart. They were first connected in series aiding and then in series opposing configurations. The error (ϵ) was calculated from the measured transfer impedances. The results are as follows: 1) unshielded core, ϵ = 63 ppm; 2) three-layer shield, ϵ = 0.01 ppm; 3) high-permeability shield as in Fig. 5(b), ϵ = 1.2 ppm.

The above results indicate that the three-layer shield is more than adequate for the elimination of magnetic error. This type of shield is used for the current comparator and the external range extender TR3 in Fig. 2. In the internal range extender (TR2) the turns are closely coupled resulting in lower magnetic errors and requiring less magnetic shielding. A two-layer enclosure consisting of high-conductivity and high-permeability shields is used in this transformer.

C. Two-Stage Transformer Networks

Shielding eliminates the magnetic errors of current comparators but not the errors of range extending transformers in Fig. 2, although in these the shielding is also required. A two-winding current transformer or an autotransformer requires flux in the core and therefore magnetizing current which causes an error in the cur-

TABLE II
Shielding Factors for Various Enclosures

Shields	Shielding Factor		
	Type of Field		
	Radial	Axial	Dipole
1	87	7.9	42
1,2	150	18	71
1, 2, 3	66,000	7,300	8,000
2	1.7	2.4	1.6
3	290	22	73
1, 3	560	48	2,700
2, 3	1100	160	220
4	8.8	2.0	45

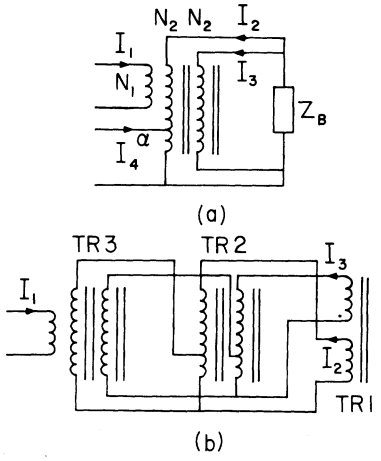

Fig. 6. Two-stage transformer. (a) Schematic diagram. (b) Interconnection of three transformers.

rent ratio. The magnetizing current can be supplied to the circuit at the output terminals with a separate current transformer, in which case the remaining error may be only a negligible second-order term. The two transformers are usually constructed as a single unit with two cores and three windings, two of which are common to both transformers. The unit is known as a two-stage transformer. The theory of two-stage transformers has been described before [8], [9]. Several important features are summarized here and an example of how to achieve current ratios as large as $10^7/1$ is provided.

A schematic diagram of a two-stage transformer is shown in Fig. 6(a). The windings at left (primary and tapped secondary) are wound on both cores while the third (compensation) winding is wound only on the inner core at right. The compensation winding and its core must be shielded by the previously described techniques. The transformer of Fig. 6(a) can be operated either as an autotransformer, or a transformer with an isolated primary winding, or simultaneously in both modes. The currents are related as follows:

$$I_2 + I_3 = -I_1\frac{N_1}{N_2}(1 + \epsilon_1) - I_4\alpha(1 + \epsilon_2) \quad (4)$$

where the errors are given by

$$\epsilon_1 = -\frac{Z_2Z_3}{Z_{m1}Z_{m2}} - \frac{Z_B}{Z_{m1}} \quad (5)$$

$$\epsilon_2 = -\frac{(\Delta Z_2)Z_3}{Z_{m1}Z_{m2}} - \frac{Z_B}{Z_{m1}} \quad (6)$$

Z_2 and Z_3 are the leakage impedances of the secondary and compensation windings; ΔZ_2 is the unbalanced leakage impedance above the tap of the secondary winding; Z_{m1} and Z_{m2} are the magnetizing impedances of the inner and outer cores.

A two-stage transformer has negligible error only if the external burden impedance Z_B which is common to the secondary and compensation windings is small, typically a few milliohms. When cascading transformers, the compensation winding can be connected to a separate circuit. In such a case the external burden impedances connected to the secondary and compensation windings are indistinguishable from the leakage impedances and a higher accuracy can be achieved. An autotransformer is more accurate than the transformer with a separate primary winding if the leakage impedances can be balanced about the tap point, i.e., if ΔZ_2 is small. This is generally not practical for ratios larger than 10/1.

The circuit of Fig. 6(b) illustrates techniques of cascading two-stage transformers. It is the actual circuit used and shows how the two range extenders and the current comparator are interconnected. Note how the compensation windings are connected to separate circuits thus avoiding common load impedances with the secondary windings. The compensation winding of TR3 in Fig. 2 is connected to a circuit which links only the inner core of TR2 to avoid a relatively large inductively coupled load impedance. However, the compensation winding of TR2 is connected to a separate winding which is wound on both cores of a two-stage (compensated) current comparator. The inductively coupled load in this case is negligible.

Two-stage transformer techniques offer other advantages, such as the transfer of the effective leakage impedance from the compensated to the uncompensated winding, for example, in Fig. 2 from the N_1 winding to the N_2 winding. However, the primary reason for compensating the current comparator in this application was to provide a low impedance path for the unbalanced harmonic currents through the compensation winding and the tuned detection winding.

D. Capacitive Errors and Sensitivity Considerations

To obtain high sensitivity and large ratio range, it is advantageous to construct the ratio windings of a current comparator with many turns; in the previous instrument 1000 turns were used [1]. A large number of turns is, however, associated with large internal capacitances and a substantial capacitive error. In this instrument the maximum number of turns in each ratio winding is nominally 100 which maintains the capacitive errors below a few parts in 10^7.

The range extenders have a few fixed ratios and therefore they can be compensated for any capacitive errors; alternatively, the bridge readings can be corrected for these errors. The internal range extender is compensated by connecting a capacitor between the tap and the common terminal. The external range extender is left intact, although its deviations from the nominal ratio are known, because the required compensating network is somewhat difficult to implement.

The major disadvantage of the reduced number of turns in a current comparator is decreased sensitivity. The bridge was designed to detect 4×10^{-10} ampere-turns—0.1 ppm when 100 V (60 Hz) was applied to a 1000-pF standard capacitor. To attain this sensitivity, the detection system was optimized to the point where the limiting factor was the thermal noise of the current comparator.

Lower thermal noise is achieved by using cores with 0.025-mm thick tape instead of the more conventional power frequency cores with 0.1-mm thick tape. By using thinner magnetic material, the Q of the core is increased from 6 to 40 with a resulting reduction in the thermal noise by a factor of 2.6. The detection winding (2200 turns) is tuned with an external capacitor to suppress harmonic currents and to provide a better match between the current comparator and high impedance detectors. The noise resulting from magnetostrictive effects can be an order of magnitude larger than the thermal noise. It is reduced to a negligible value by mounting the current comparator in a resilient medium and by demagnetizing the core before critical applications.

In the tuned condition the impedance of the detection winding is 4.4 mΩ which for an unbalance of 4×10^{-10} ampere-turns produces a 0.8-μV signal, well above the thermal noise of 0.27 $\mu V/\sqrt{Hz}$. The signal, before being passed to a commercial null detector, is first amplified in a battery-operated preamplifier: The field effect transistor in the preamplifier input stage has a noise level of 0.05 $\mu V/\sqrt{Hz}$.

E. Amplifier Circuits

As seen from Fig. 2, the bridge contains four amplifier circuits. These circuits do not primarily affect the bridge accuracy. In the case of amplifiers 1 and 2, a small signal is generated to balance the loss component. Similarly, amplifiers 3 and 4 remove small residual effects of lead and internal bridge impedances. Any error in the amplifier output becomes a second-order error in the bridge reading. Nevertheless, moderately high gains and stable computing impedances are required, especially in amplifiers 1 and 2 since it is desirable to measure the loss component with a 0.1-percent accuracy.

At first glance the amplifier circuits in Fig. 2 may appear trivial. However, considerable effort was required to achieve stable operation and sufficiently high gain in amplifier 1. The difficulty arises because a gain of the order of 10 000 is required at the principal operating frequencies of 50 and 60 Hz. At about 1 Hz the phase shift of the feedback loop exceeds 180° which leads to a potentially unstable system. A somewhat unconventional stabilizing technique was employed.

An equivalent block diagram of amplifier 1 with some detail included is shown in Fig. 7. A is the gain of the operational amplifier; H_1 is the transfer function of a parallel compensating (local feedback) network which itself contains an amplifier; H_3 is the transfer function of a series compensating network and the power amplifier stage. Let H_2 be the transfer characteristic of the entire principal feedback path via H_3 and C_f. Stability difficulties at low frequencies arise from the 180° phase shift produced by the blocking capacitor (C_B) and the transformer; an additional phase shift of up to 90° is caused by C_f and $2G_s$.

The gain in the frequency band between 1 and 50 Hz cannot be rolled off to one with a series compensating network without encountering phase shifts in excess of 180° and hence stability problems. Instead the system is stabilized with the parallel feedback network. The characteristics of the various parts of the amplifier circuit are presented as Bode plots in Fig. 8.

In the frequency band between 50 and 400 Hz the gain of the parallel compensating network is less than −80 dB and, therefore, negligible. The principal feedback path (H_2) is the dominant one. Outside the region of the operating frequencies the gain of H_1 is increased rapidly at 60-dB per decade until the compensating network becomes the dominant feedback path. At this point the gain of H_1 is kept constant with negligible phase shift. It should be noted that the amplifier is not stable with the principal feedback loop open. The compensating networks are carefully designed and constructed to yield the desired characteristics. The parallel compensating network is a triple lead-lag network.

Amplifier 3 in Fig. 2 was stabilized with a similar technique. Amplifiers 2 and 4 utilize conventional operational amplifier circuits.

CALIBRATION

A significant portion of the bridge development involved the verification of its accuracy. The calibration was difficult because it required measurements with state-of-art accuracy and sufficiently stable transfer standards of ratio. These requirements limited the number of available methods. Two measurement procedures were developed for this task—one to verify the accuracy of individual transformers before they were installed in the bridge; the other, to calibrate the final bridge assembly.

A. Transformer-Type Calibrating Network

Calibration of isolated transformers was considered desirable to verify the computed limits of ratio errors. A self-contained procedure based on a linear transformer type network was employed. A simpler version of this method was previously used to calibrate isolated induc-

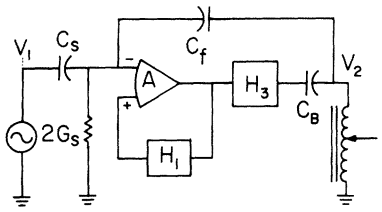

Fig. 7. Detailed diagram of amplifier 1.

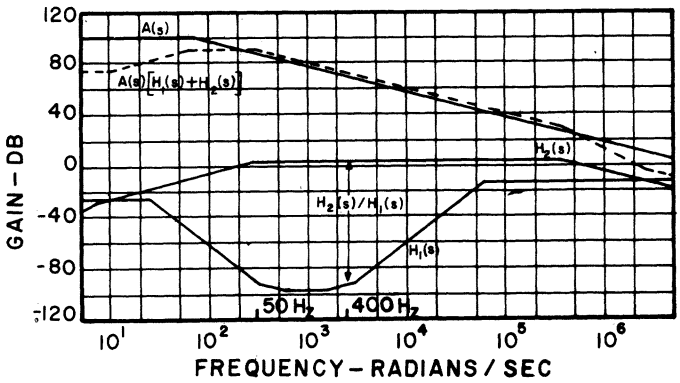

Fig. 8. Frequency response of components of amplifier 1.

tive divider decades or autotransformers with 10 equal sections [10].

The circuit for calibrating a current comparator is shown in Fig. 9. The basic calibrating network is in the area circumscribed by the broken lines. It consists of an ideal 1/1 current comparator at left, a 10/1 current transformer at right, and a small transformer to supply the current to the error network (EN) for balancing the bridge. Before the calibration, the 1/1 current comparator is made "ideal"—I_2 is always equal to I_1—by adjusting internally connected capacitances to balance out the effects of inherent stray capacitances. The current transformer has a very stable ratio which is unaffected by the magnitude of the current, but this ratio does not have to be adjusted exactly equal to the nominal value. The amplifier circuit essentially eliminates the impedance to I_3 and I_4.

The network is balanced by adjusting the variable source at right and the error network to produce null at both detectors. Initially the calibrator is connected to the common and 0.1 taps, and the readings of the error network are noted. Then it is moved to the 0.1 and 0.2 taps and the procedure is repeated. From these two measurements the corrections of the 0.1 tap as well as the 10/1 transformer are obtained in terms of the correction to the 0.2 tap. The procedure is continued for all the adjacent pairs of taps yielding the necessary corrections and accurately known ratios for any combination of two taps.

The ten sections in the lower 100-turn ratio winding (N_2 in Fig. 2) were also calibrated by this procedure. The tie between the upper and lower windings was obtained by a 1/1 comparison. For this, one of the windings in the current comparator of the calibrator was reversed, i.e., I_1 and I_2 were in the same direction. All ten

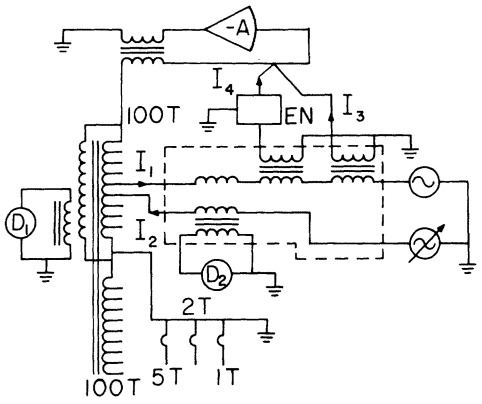

Fig. 9. Transformer-type calibrating network.

terminals in the lower winding were brought out for the purpose of the calibration. In the actual bridge, taps are available only at 100, 50, 20, and 10 turns.

In addition to the 100-turn windings, the current comparator has taps at 5, 2, and 1 turn resulting in range multipliers of ×20, ×50, and ×100. These were also calibrated by the same procedure, except that I_4 and I_3 were injected in an intermediate tap of the upper winding. For example, when comparing 0.1 and 0.05 taps, I_3 and I_4 were supplied to the 0.5 tap. To compare the 0.05 tap with the smaller ones, a temporary 3-turn winding was placed on the current comparator.

The results indicate that the ratio errors of all combinations of taps within one winding, either the upper or lower are within 0.1 ppm. However, the difference between the two windings is about 0.3 ppm for the quadrature component; the in-phase error is negligible. This error is believed to be of capacitive origin. Its direction is as expected for a compensated current comparator.

The 10/1 taps in both range extenders were calibrated on a relative basis against a previously calibrated 10-tap inductive divider. The calibrating network of Fig. 9 was also adapted for this purpose. The errors of the internal range extender after compensation with a capacitor were negligible, but the errors of the external extender were about 0.2 and 0.5 ppm for the in-phase and quadrature components, respectively.

B. Capacitor Method

Another self-contained procedure was employed for the final calibration after the bridge was fully assembled. A group of capacitors was utilized to form intermediate transfer standards of ratio. The ratio involving an uncalibrated tap was measured against a known transformer ratio using a pair of capacitors. Except for the ratios of 1/1, 2/1, and 2.5/1, this method did not rely on connecting in parallel individually calibrated capacitors to produce large ratios. In fact the largest bridge ratios were calibrated using a 1 to 10-μF capacitance decade box. Parallel connection of individually calibrated large capacitors would not be feasible.

The procedure is illustrated with an example. Consider the current comparator in Fig. 10. The detection winding is at the left. Assume that the ratios of all taps,

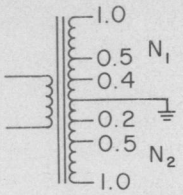

Fig. 10. Necessary taps in current comparator to calibrate 5/1 ratio.

except the 0.2 tap of N_2, have already been measured with respect to each other. For these previous measurements nominally equal capacitors were connected in parallel. The ratios involving the 0.2 tap of N_2 are determined by first measuring the ratio $N_1/N_2 = 0.4/0.2$. A convenient capacitance ratio 1000 pF/2000 pF can be utilized. This capacitance ratio is then measured against the turns ratio $N_1/N_2 = 1.0/0.5$. Since from the previous measurements the ratio 1.0/0.4 in the N_1 winding is known, the correction to $N_1/N_2 = 1.0/0.2$ can be computed. Thus an accurate 5/1 ratio is obtained.

The next step is to calibrate ratios associated with the 0.1 tap of N_2, which is not shown in the diagram. For this a 5/1 capacitance ratio which can be measured directly with the bridge is used. Following this the ratio $N_1/N_2 = 0.5/0.1$ is measured and $N_1/N_2 = 1.0/0.1$ computed.

The results obtained by this procedure are tabulated in Table III. The corrections for the lower ratios are well within 1 ppm. The estimated uncertainty of this method is 0.1 ppm for the two lowest ratios of 1/1 and 2/1. From then on each successive step contributes another 0.1 ppm of uncertainty. Combining them as the square root of the sum of the squares, the uncertainty for the 1000/1 ratio, for example, is $\sqrt{9} \times 0.1$ ppm = 0.3 ppm.

The problem of this calibration method is the accumulation of errors at higher ratios. It is believed that a higher calibration accuracy would be warranted by the direct reading accuracy capability of the bridge. The consistently low corrections in Table III suggest that the estimate of uncertainties may be too pessimistic.

TABLE III
Calibration of Bridge at 60 Hz

M	α (ppm)	β (ppm)
1	0	−0.3
2	+0.1	−0.1
5	+0.1	0
10	+0.2	0
20	+0.3	+0.2
50	+0.3	+0.2
100	+0.3	+0.2
200	+0.3	+0.1
500	+0.4	0
1000	+0.5	+0.1
2000	+0.4	−0.6
5000	+0.4	−0.6
10, 000	+0.4	−0.6
20, 000	+0.3	+0.4

$Y_x/Y_s = M(1 + \alpha - j\beta)$
Y_x/Y_s = measured admittance ratio
M = nominal ratio or bridge setting
α = in-phase correction
β = quadrature correction

APPLICATIONS

The assembled bridge is shown in Fig. 11. The transformers are mounted in the chassis behind the lower panel while the electronic components, including the inductive divider for the dissipation factor control, are installed behind the upper panel.

The bridge has been in use at NBS for the past five years. It is the primary ratio standard for most measurements at high alternating voltages, which include impedance measurements on standard compressed-gas capacitors, large power-factor-correction capacitors, high-voltage inductors (shunt reactors), and dielectric samples; voltage-ratio measurements of voltage transformers and other types of high-voltage dividers.

While a few measurements require accuracies approaching the capability of the bridge, most are of the type requiring a few tens of ppm accuracy. The relative-

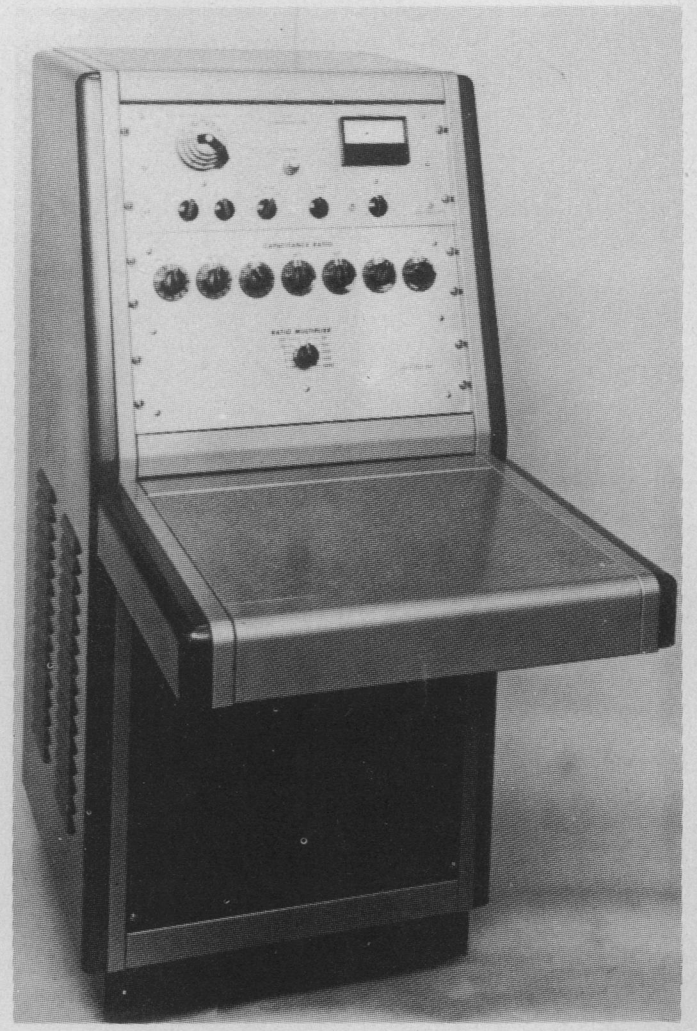

Fig. 11. Bridge assembly.

ly small and compact construction, the direct reading feature, and the simplicity of connections also make it convenient for these lower accuracy measurements.

This development resulted in a practical instrument which improved the state-of-art accuracy of high-voltage capacitance measurements by an order of magnitude. This accuracy is more than adequate for engineering applications in which most high-voltage measurements fall. In fact, the accuracy and sensitivity of the bridge are such that it can compete successfully with bridges based on three-winding voltage transformers for calibration of commercially available low voltage standard capacitors at voltages above 100 V.

The development also demonstrated the accuracy capabilities and limitations of low-level adjustable-range current comparators with large ratios. While a ppm accuracy without corrections was achieved, the possibility for a further significant increase appears unlikely. The limitation is imposed by the internal capacitance. If still greater accuracy is required, a current comparator with a few fixed ratios to which corrections are applied will have to be used.

Finally, the investigation clarified causes of magnetic errors and suggested concepts for the design of highly effective magnetic shields. The magnetic error can be reduced to a 0.01-ppm level with elaborate multilayer shields. It can also be reduced by proper selection of cores.

ACKNOWLEDGMENT

The authors acknowledge the assistance of M. C. Cutkosky for calibrating the bridge, E. D. Sims for preparing the diagrams, and J. Cunningham for typing the manuscript.

APPENDIX
BASIC BRIDGE SPECIFICATIONS

Capacitance ratio range:	1/1 to 10^4/1 with the internally installed transformers; to 10^7/1 with the external range extender
Dissipation factor range:	−0.01 to +0.01
Frequency:	Optimum 50 to 60 Hz; with reduced accuracy to 400 Hz
Standard capacitor:	External and not a part of the bridge; optimum values 100 to 1000 pF, but the bridge will function with other values
Voltage:	Determined by the voltage rating of the two capacitors and the current rating of the bridge
Current:	In the standard capacitor, 10-mA maximum; in the unknown capacitor with the internal transformers 1 A; with the external transformer, 1000 A.
Readout:	Direct reading in capacitance ratio and dissipation factor (at 60 Hz).
Resolution:	Capacitance ratio 0.1 ppm to 0.25 ppm; dissipation factor 10^{-7}.
Sensitivity:	Can detect 4×10^{-12} A unbalance in the standard capacitor.
Accuracy:	1. Ratio multiplier settings from ×1 to ×1000—capacitance ratio ±1 ppm, DF $\pm 10^{-6}$ 2. Ratio multiplier settings from ×2000 to $\times 10^5$—capacitance ratio ±2 ppm, DF $\pm 2 \times 10^{-6}$ 3. Ratio multiplier settings from $\times 2 \times 10^5$ to $\times 10^7$—capacitance ratio ±3 ppm, DF $\pm 3 \times 10^{-6}$

REFERENCES

[1] N. L. Kusters and O. Petersons, "A transformer-ratio-arm bridge for high-voltage capacitance measurements," *IEEE Trans. Commun. Electron.*, vol. CE-82, pp. 606–611, Nov. 1963.
[2] O. Petersons, "A transformer-ratio-arm bridge for measuring large capacitors above 100 volts," *IEEE Trans. Power App. Syst.*, vol. PAS-87, pp. 1354–61, May 1968.
[3] R. D. Cutkosky, "Techniques for comparing four-terminal-pair admittance standards," *J. Res. Bur. Stand. C, Eng. Instrum.*, vol. 74C, nos. 3 and 4, pp. 63–78, July–Dec. 1970.
[4] O. Petersons, "A wide-range high voltage capacitance bridge with one ppm accuracy," D.Sc. dissertation, School of Engineering and Applied Science, George Washington Univ., Washington, D. C., Feb. 1974.
[5] N. L. Kusters, "The precise measurement of current ratios," *IEEE Trans. Instrum. Meas.*, vol. IM-13, pp. 197–209, Dec. 1964.
[6] G. H. Rayner, "Flux pattern in spiral tape cores," *J. Sci. Instrum. (J. Phys. E)*, vol. 1, p. 780, 1968.
[7] H. Kaden, *Wirbelstroeme und Schirmung in der Nachrichtentecknik*, Berlin, Germany: Springer--Verlag, 1959.
[8] H. B. Brooks and F. C. Holz, "The two-stage current transformer," *Trans. Amer. Inst. Elect. Eng.*, vol. 41, pp. 382–391, June 1922.
[9] O. Petersons, "A self-balancing current comparator," *IEEE Trans. Instrum. Meas.*, vol. IM-15, pp. 62–71, Mar./June 1966.
[10] O. Petersons and W. C. Sze, "Calibration of transformer ratios with a reciprocal transformer-type network," in *Conf. Dig., Conf. Precision Electromagnetic Measurements*, pp. 57–59, June 1970.